

# Microwave assisted rapid and complete degradation of atrazine using TiO<sub>2</sub> nanotube photocatalyst suspensions

Gao Zhanqi, Yang Shaogui\*, Ta Na, Sun Cheng

State Key Laboratory of Pollution Control and Resources, School of the Environment,  
Nanjing University, Nanjing 210093, China

Received 15 September 2006; received in revised form 16 November 2006; accepted 16 November 2006  
Available online 25 November 2006

## Abstract

A technology, microwave-assisted photocatalysis on TiO<sub>2</sub> nanotubes, which can be applied to degrade atrazine rapidly and completely, was investigated. TiO<sub>2</sub> nanotubes were prepared, and confirmed by XRD, TEM and ESR. Microwave-assisted photocatalytic degradation of atrazine in aqueous solution was investigated. The result indicates that atrazine is completely degraded in 5 min and the mineralization efficiency is 98.5% in 20 min, which is obviously more efficient than that by the traditional photocatalytic degradation methods. It may be attributed to the intense UV radiation generated by electrodeless discharge lamps under microwave irradiation, the increased number of •OH, additional defect sites on TiO<sub>2</sub> under the irradiation of microwave and larger specific surface area of TiO<sub>2</sub> nanotubes which could adsorb more organic substances to degrade than TiO<sub>2</sub> nanoparticles. Along with the degradation of atrazine, the concentrations of Cl<sup>-</sup> and NO<sub>3</sub><sup>-</sup> increase gradually. In 20 min [Cl<sup>-</sup>] and [NO<sub>3</sub><sup>-</sup>] are 3, 27.8 mg/L, respectively, which are close to their stoichiometric values. The major intermediates of atrazine were identified by HPLC/MS and possible degradation pathways of atrazine in microwave-assisted photocatalysis on TiO<sub>2</sub> nanotubes were proposed.

© 2006 Elsevier B.V. All rights reserved.

**Keywords:** Atrazine; Nanotubes; Microwave; Photocatalysis

## 1. Introduction

Atrazine [2-chloro-4-(ethylamino)-6-(isopropylamino)-S-triazine] is widely used for weed control in the cultivation of corn and other crops. Although many European countries have banned its use, atrazine are still used in other countries, such as china, USA [1] and so on. Due to its high aqueous solubility and high mobility, atrazine is frequently detected in surface and ground waters, which leads to environmental problems. Therefore, the search for effective remediation methods of removing atrazine from water is important [2].

The degradation and purification methods for polluted waters include using various adsorbents [3], such as activated carbon [3], microbial action [4] and chemical oxidation [5]. However, each method has its own limitations and disadvantages. Adsorption cannot degrade pollutants which just transfers their phase

[3]. Microbial processes are typically very slow and sometimes inefficient and the disposal of activated sludge must to be considered [4]. Chemical oxidation is unable to mineralize all organic substances [5].

Advanced oxidation processes (AOPs) have been used to degrade atrazine too, including UV/H<sub>2</sub>O<sub>2</sub> [6], Fenton reagent [7], and TiO<sub>2</sub>-supported UV photolysis [8–10]. Among AOPs, TiO<sub>2</sub>-supported UV photolysis has been proven effective in degrading atrazine through de-chlorination, de-alkylation and de-amination processes [8–10]. However, cleavage of the triazine ring was not observed. Further, cyanuric acid (CA) was formed as an end product in the degradation of atrazine on TiO<sub>2</sub> [8–10].

And in the application of TiO<sub>2</sub>, there are still some problems to be solved, such as its low specific surface area and poor quantum efficiency. To improve its photocatalytic activity, TiO<sub>2</sub> was modified with various methods, including modification for harvesting visible light [11] and enlarging surface area [12,13]. Compared with TiO<sub>2</sub> nanoparticles, TiO<sub>2</sub> nanotubes have larger surface area, so it is expected to improve the activity of photocatalyst [12,13]. In addition, photocatalysis assisted

\* Corresponding authors. Tel.: +86 25 83593239; fax: +86 25 83593239.  
E-mail addresses: [yangdlut@126.com](mailto:yangdlut@126.com) (Y. Shaogui),  
[chengsun@publicl.ppt.js.cn](mailto:chengsun@publicl.ppt.js.cn) (S. Cheng).

by microwave powered electrodeless discharge lamps (EDLs) has been used to treat polluted waters recently and it has been known that microwave irradiation not only can excite EDLs to generate ultraviolet–visible (UV–vis) radiation which can excite  $\text{TiO}_2$  for photocatalysis, but also could significantly improve the photocatalytic efficiency of  $\text{TiO}_2$  for removal of pollutants [14,15]. Therefore, microwave-assisted photocatalysis on  $\text{TiO}_2$  nanotubes with larger surface area may have better capacity to degrade pollutants.

The main objective of present study is to investigate the degradation of atrazine by microwave-assisted photocatalysis on  $\text{TiO}_2$  nanotubes and propose the possible photocatalytic degradation pathways of atrazine.

## 2. Experimental

### 2.1. Materials

The reagents used were atrazine (97.4% purity, Sigma–Aldrich), tetrabutylortho titanate (CP, Tianjin Chemical Company), NaOH (AR, Lingfeng Chemical Company), HCl (AR, Nanjing Chemical Company).

### 2.2. Preparation of $\text{TiO}_2$ nanotubes

$\text{TiO}_2$  nanotubes were prepared by hydrothermal processing method according to previous report [16].  $\text{TiO}_2$  particles were prepared by ultrasound assisted tetrabutylortho titanate hydrolysis. Then, 1 g  $\text{TiO}_2$  particles were put into a Teflon vessel with 35 mL 10 M NaOH solution. The vessel was placed in a stainless steel vessel and held at 130 °C for 24 h in the muffle furnace. The obtained powders were washed well with 0.1 M HCl solution and distilled water until pH of the solution was about 7. The sample was dried at 80 °C for 10 h and then calcined at 400 °C for 1 h.

### 2.3. Characterization of $\text{TiO}_2$ nanotubes

The morphology of the  $\text{TiO}_2$  nanotubes was characterized by transmission electron microscopy (TEM; Hitachi-600). The crystallinity of the  $\text{TiO}_2$  nanotubes was determined by X-ray diffraction (XRD) using a diffractometer with Cu KR radiation (Model, Shimadzu LabX XRD-6000). The  $\bullet\text{OH}$  forming on the surface of  $\text{TiO}_2$  nanotubes was trapped using the DMPO spin-trap technique and analyzed by JEOL JES-TE200 ESR spectrometer.

### 2.4. Microwave-assisted photocatalytic experiment

The photocatalytic experiments were conducted using a microwave powered EDLs system [17] under the following conditions: the Bunsen beaker was filled with 50 mL 20 mg/L aqueous solution of atrazine and the initial pH was 8.1. Then two EDLs containing mercury vapor with a peak emission at 254 nm and 0.05 g  $\text{TiO}_2$  nanotubes were placed into the reactor vessel. The reaction times were scheduled.

## 2.5. Analytical methods

The samples after reaction were filtered with 0.20  $\mu\text{m}$  Millipore to remove catalysts. The determination of atrazine concentrations was performed by HPLC. The HPLC evaluation was carried out using a C18 column (4.6  $\times$  250 mm, Agilent), methanol/ $\text{H}_2\text{O}$  = 80:20 (v/v) as mobile phase with a flow rate of 1 mL/min and a detection wavelength of 223 nm. The solution pH was measured with pH meter (PHS-2C, China). The variations of  $\text{Cl}^-$  and  $\text{NO}_3^-$  concentration in reaction system were measured by chloride ion-selective electrode (pCl-1, China) and ultraviolet spectrophotometer (V2550, Japan) at 207 nm, respectively. The intermediates were detected by HPLC/MS (Thermo, USA) equipped with an atmospheric pressure chemical ionization interface (APCI). The samples were chromatographically separated using a Beta Basic-18 column (150  $\times$  2.1 mm) at a flow rate of 1.0 mL/min under isocratic conditions. The ion mode was set on positive mode. The mobile phase was methanol–water (60:40, v/v). Twenty microlitres of extract was injected using the auto sampler.

## 3. Results and discussion

### 3.1. Morphology of $\text{TiO}_2$ nanotubes and XRD analysis

TEM image of  $\text{TiO}_2$  nanotubes after calcinations at 400 °C for 1 h illustrates they are tubular structure (shown in Fig. 1), which is similar to that of  $\text{TiO}_2$  nanotubes prepared by other studies using hydrothermal method [16,18,19]. The tops of the tubes are open. Their diameter and length are about 10 and 200 nm, respectively.

Fig. 2 is XRD profile of the  $\text{TiO}_2$  nanotubes. An anatase phase corresponding to 25.3° appears in the XRD patterns and the diffraction peak is intensive. The average crystalline size

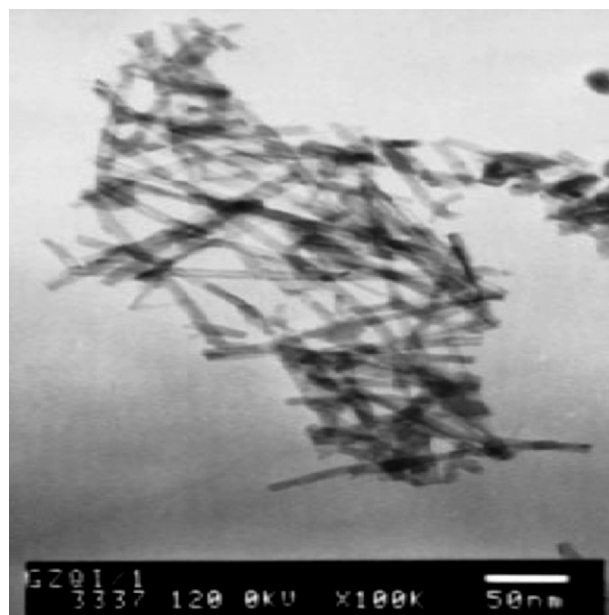


Fig. 1. TEM image of  $\text{TiO}_2$  nanotubes (100 $\times$ ).

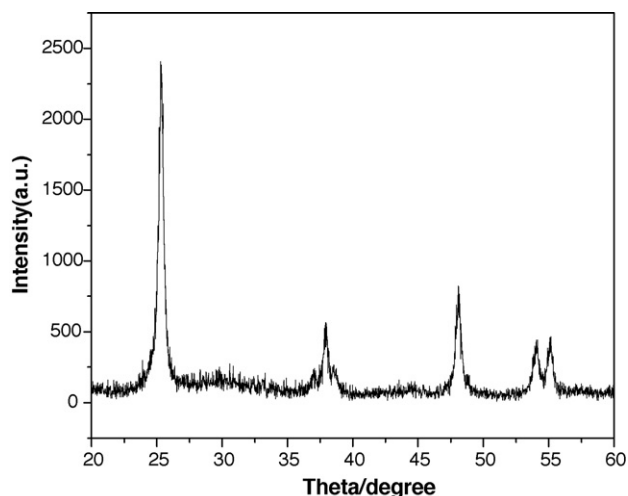
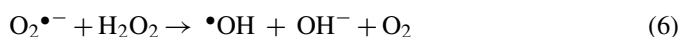
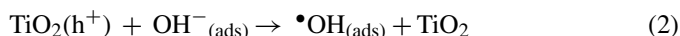


Fig. 2. XRD spectrum of TiO<sub>2</sub> nanotubes.

calculated using a diffraction peak from Scherer's formula was about 2.8 nm.

### 3.2. ESR analysis

When TiO<sub>2</sub> is excited under UV radiation generated by EDLs in the microwave field, photoinduced electrons (e<sup>-</sup>) and positive holes (h<sup>+</sup>) is generated. Positive holes (h<sup>+</sup>) reacts with OH<sup>-</sup> and photoinduced electrons (e<sup>-</sup>) reacts with O<sub>2</sub> adsorbed on the surface of TiO<sub>2</sub> to produce •OH (Eqs. (1)–(6)). The energy of •OH is 402.8 MJ/mol, which can destruct C–C, C–H, C–N, C–O, N–H and so on. OH radicals play an important role in the photocatalytic process. ESR spin-trap technique with DMPO is widely employed to measure the •OH forming on the surface of TiO<sub>2</sub> in present study [20,21], although the formation of O<sub>2</sub>•<sup>-</sup>/OOH• radicals had been reportedly evidenced using luminol [22]. In ESR method, DMPO can trap OH radicals at once to form the stable DMPO•OH adduct. According to the characteristic four peaks of DMPO•OH adduct in the ESR signal, it can confirm the formation of •OH [18]



The ESR spectra of different conditions are shown in Fig. 3. There are no obvious signals in the dark (without UV radiation) and DMPO alone. Comparatively, in TiO<sub>2</sub> nanotubes-DMPO, the characteristic four peaks with intensity 1:2:2:1 are observed in the ESR signal, which is agreement with reports about the •OH adduct [20]. This confirms the formation of •OH on TiO<sub>2</sub> nanotubes under the irradiation of UV radiation.

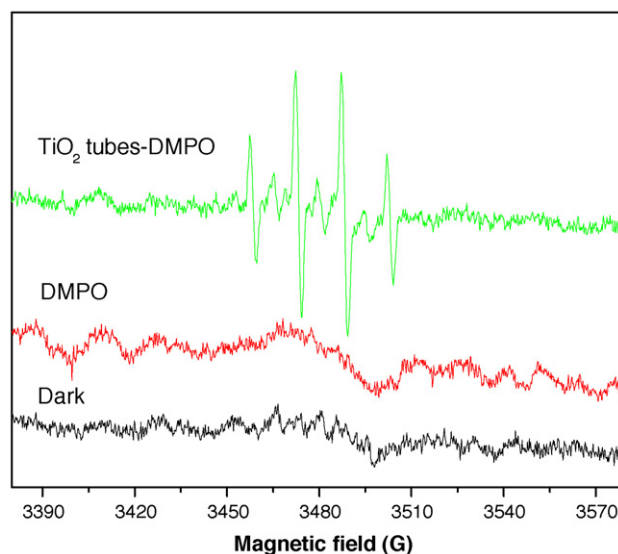


Fig. 3. ESR signal of different systems.

### 3.3. Microwave-assisted photocatalytic degradation of atrazine on TiO<sub>2</sub> nanotubes

The degradation of atrazine in aqueous solution in microwave-assisted photocatalytic process (MPC) and microwave-assisted photolytic process (MDP) was studied and the results were presented in Fig. 4. According to previous studies, photolysis of atrazine can occur under the UV radiation at 254 nm [23,24], so UV light generated by EDLs in the microwave field can degrade atrazine directly. As shown in Fig. 4, in MDP, the degradation efficiency of atrazine is 68.9% in 5 min. Since the energy of microwave radiation ( $E = 0.4 - 40 \text{ kJ mol}^{-1}$  at  $\nu = 1 - 100 \text{ GHz}$ ) is insufficient to disrupt bonds of common organic molecules [25], the degradation of atrazine can be attributed to the photolysis under UV radiation. In contrast to MDP, The presence of TiO<sub>2</sub> nanotubes results in the improvement of the decomposition of

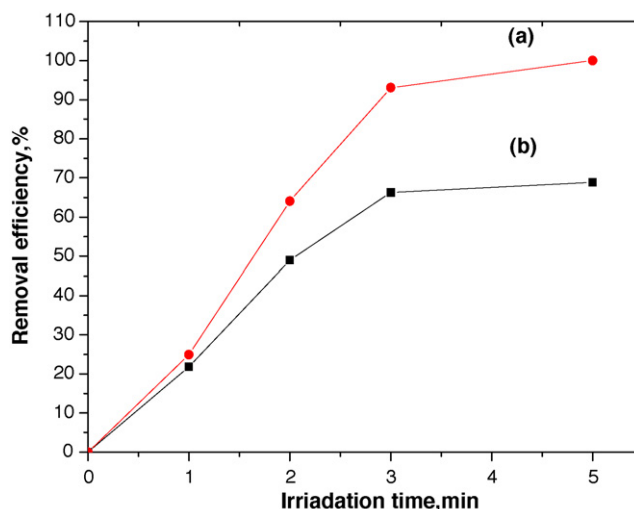


Fig. 4. Removal efficiency of atrazine in different processes: (a) MPC and (b) MDP.

atrazine. In MPC, atrazine was completely degraded in 5 min. Claudia [26] investigated the photodegradation of 21.5 mg/L atrazine in TiO<sub>2</sub> nanoparticles suspensions and found that atrazine was completely degraded after 4 h. Sandra [10] also found that the complete photodegradation of 20 mg/L atrazine in TiO<sub>2</sub> nanoparticles suspensions was gained in about 45 min. The microwave-assisted photodegradation of atrazine is much faster than previous photocatalytic degradation methods, comparatively.

### 3.4. The variation of COD<sub>Cr</sub> in MPC

The intermediates generated during the early phase of atrazine photocatalytic oxidation were proved to be toxic [27] and an increase of biotoxicity was observed under photo-Fenton/ozone treatment [28] in the first 60 min. So it is important to investigate the mineralization of atrazine for its removal from polluted water.

Several studies demonstrated that atrazine was degraded through de-chlorination, de-alkylation and de-amination, but no *S*-triazine ring was opened by •OH attacking. Furthermore, cyanuric acid (2,4,6-trihydroxy-*S*-triazine) has been detected as the final oxidation product, especially in the presence of TiO<sub>2</sub> suspensions, and no further degradation occurs because of its stability to •OH attacking [8–10]. The *S*-triazine ring opening, leading to atrazine complete mineralization, could be achieved only under hydrothermal conditions and in supercritical water media [29], which can hardly be employed in routine water treatments. Thus no effective mineralization of atrazine has been gained in the routine water treatments, even when atrazine is completely degraded. Chan [27] investigated the TOC removal in the photocatalytic degradation in P25 suspensions and found that the TOC removal increased until all alkylated side chains of atrazine were mineralized. However, only about 40% of TOC remained even after atrazine was completely degraded. Sandra [10] also found that the mineralization of the atrazine was only about 10% when atrazine was completely degraded (in about 45 min) during the photodegradation of atrazine on TiO<sub>2</sub>. And the mineralization was not improved even when the pho-

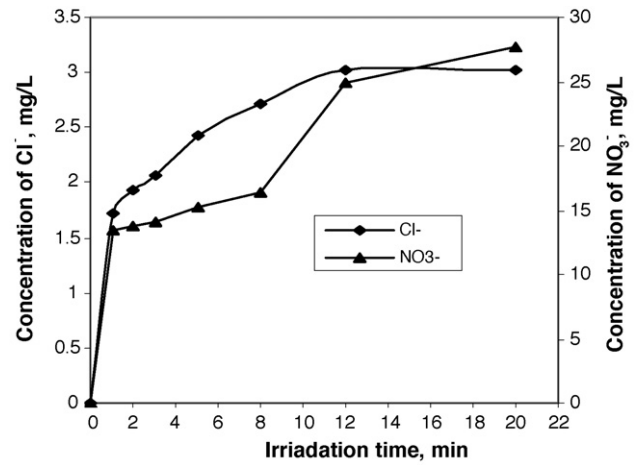


Fig. 6. The variations of Cl<sup>-</sup> and NO<sub>3</sub><sup>-</sup> in MPC.

totreatment time was extended further. However, the effective mineralization of atrazine was achieved in this study. As shown in Fig. 5, the COD<sub>Cr</sub> removal of atrazine is 98.5% in the photocatalytic degradation in MPC in 20 min, which is much higher than that in the tradition photocatalytic oxidation methods.

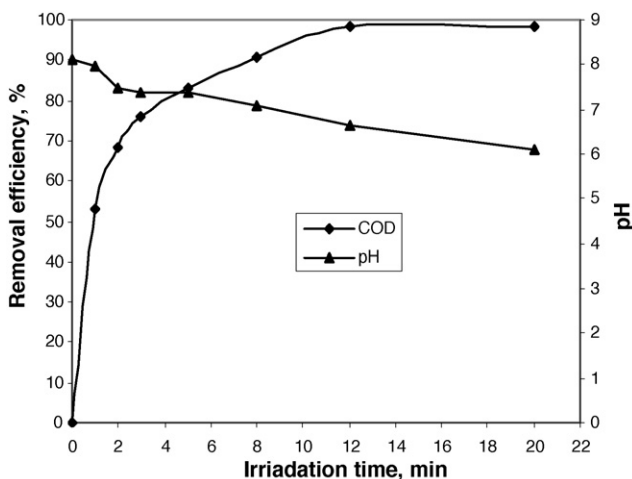


Fig. 5. The variations of COD<sub>Cr</sub> and pH in MPC.

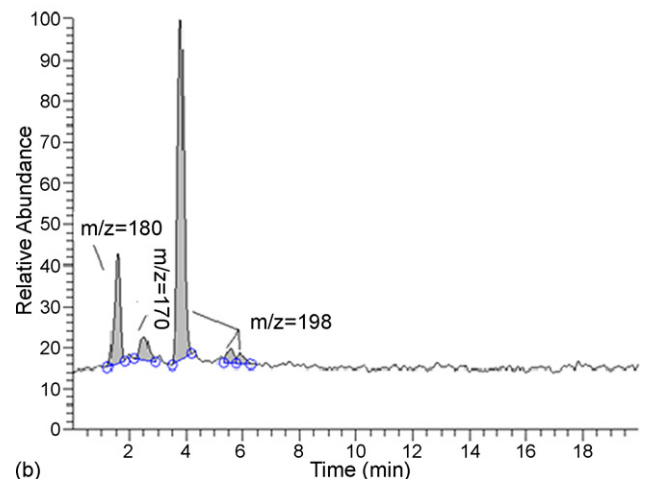
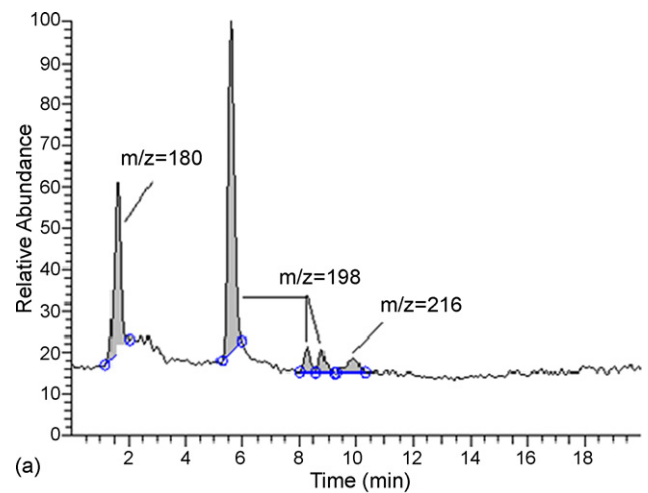


Fig. 7. HPLC/MS analysis of intermediates of atrazine in MPC: (a) 2 min and (b) 5 min.

On the basis of the results mentioned above, microwave-assisted photodegradation of atrazine is more efficient than its classical photocatalytic degradation. The possible reasons are as follows:

- (1) UV radiation generated by the EDLs in the microwave field not only can directly destroy atrazine by bond cleavage but also excite  $\text{TiO}_2$  nanotubes to produce  $\text{h}^+$  and  $\bullet\text{OH}$  on the surface, which could oxidize atrazine effectively.
- (2) The surface of  $\text{TiO}_2$  nanotubes becomes more hydrophobic under microwave irradiation and UV–vis light, which can increase the population of  $\text{OH}^-$  or  $\text{O}_2$  that can be oxidized to  $\bullet\text{OH}$  [30], therefore the number of  $\bullet\text{OH}$  increases. Horihoshi [21] has proved using ESR that there are about 20% more  $\bullet\text{OH}$  generated by microwave-assisted photocatalysis than traditional photocatalysis.  $\bullet\text{OH}$  has strong oxidizing ability and can destruct any bond of organic molecules in theory, the abundant  $\bullet\text{OH}$  may lead to the open of *S*-triazine ring in 20 min, although cyanuric acid as the final oxidation product is stable to  $\bullet\text{OH}$  attacking in precious studies during their reaction time [8–10]. Horikoshi. [21] investigated the mineralization of PyroninB (PyB) on microwave/photocatalytic method in the presence of  $\text{TiO}_2$  particulates (PD/MW) and traditional photocatalysis on  $\text{TiO}_2$  (PD) and found that the mineralization of PyB reached 77% on PD/MW and was 2.3 times higher than that on PD in 3 h which was only 12.8%. And desorption of water molecules on the surface of  $\text{TiO}_2$  also provides more active sites of the reactants to attach for oxidation [31].

- (3) Microwave could generate additional defect sites on  $\text{TiO}_2$ , increase the transition probability of  $\text{e}^- - \text{h}^+$  and decrease the  $\text{e}^- - \text{h}^+$  recombination on  $\text{TiO}_2$  surface [32].
- (4)  $\text{TiO}_2$  nanotubes have larger specific surface area than  $\text{TiO}_2$  nanoparticles, which could adsorb more organics to degrade which may imply an increase in the activity.

During the degradation of atrazine on  $\text{TiO}_2$ , organic acids with small molecules and  $\text{CO}_2$  could be produced, which can decrease pH of reaction solution. As shown in Fig. 5, pH decreases from 8.1 to 7.1 in 20 min

The de-chlorination occurs during the degradation of atrazine. The concentration of  $\text{Cl}^-$  increases to 3 mg/L (shown in Fig. 6) in 20 min. In the de-amination and *S*-triazine ring opening processes,  $\text{NO}_3^-$  is generated and the concentration of  $\text{NO}_3^-$  increases to 27.8 mg/L (shown in Fig. 6). Both dates are close to their stoichiometric values (3.3 and 28.7 mg/L, respectively).

### 3.5. Identification of intermediates by HPLC/MS in MPC

The intermediates of atrazine in the reaction time of 2 and 5 min were identified by HPLC/MS and the results are shown in Fig. 7. In 2 min, four major intermediates were detected: 4-ethylamino-6-isopropylamino-*S*-triazine (EIST) and 2-hydroxy-4-ethylamino-6-isopropylamino-*S*-triazine (OIET), 2-hydroxy-4-ethylamino-6-(*N*-methyl-acetamide)-*S*-triazine (ODET), 2-hydroxy-4-methylamino-6-(1-methyl-1-ethanol)-*S*-triazine (HAET). In 5 min, besides the four intermediates above, 2-hydroxy-4-ethylamino-6-hydroxyl-*S*-triazine (ADE) was detected. On the basis of the intermediates described above,

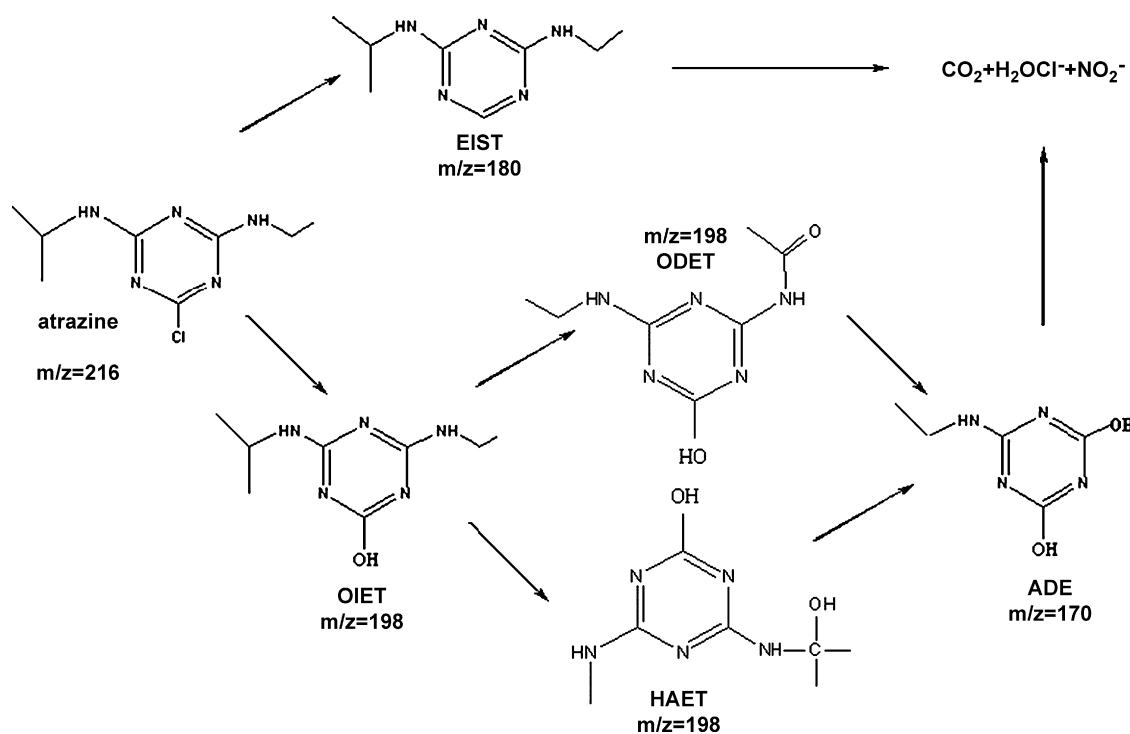


Fig. 8. The possible degradation pathways of atrazine in MPC.



possible degradation pathways of atrazine in MPC are proposed (shown in Fig. 8):

- (1) Direct photolysis of atrazine under the UV radiation generated by EDLs in the microwave field. According to previous studies [22,23], UV radiation would result in the decomposition of organic molecules by bond cleavage and free radical generation, but usually it occurs slowly. However, based on the data about the degradation of atrazine in MPC (shown in Fig. 4), atrazine is effectively degraded. The photolysis of atrazine under UV radiation may also play an important role in the degradation of atrazine in MPC. The mechanism about photolysis of atrazine under the UV radiation has been studied well previously [22,23]. Claudia et al. [26] proposed the mechanism of photolysis at 254 nm that the first step is fast de-chlorination to with its consequent almost complete transformation into OIET and then followed by slow de-alkylation. However, a new intermediate EIST, which was not reported in previous studies is detected. It may arise from that C–Cl bond of atrazine directly cleaves by the intense UV radiation generated by EDLs.
- (2) Photocatalytic degradation of atrazine on TiO<sub>2</sub>. Valence band holes (h<sup>+</sup>), generated on the surface of, TiO<sub>2</sub>, can oxidize either adsorbed organic molecules directly, or OH<sup>-</sup> or O<sub>2</sub> adsorbed on the semiconductor surface, yielding •OH, which are also able to attack and oxidize organic substrates. Although two oxidation paths can hardly be distinguished in most cases, •OH are expected to be the main responsible for atrazine degradation [26]. Because the breaking of C–Cl bond is energetically most favorable, de-chlorination could be the first step and then followed by de-alkylation.

Photolysis and photocatalysis are in coexistent during the degradation of atrazine in MPC, and intermediates may be generated by one or both of the two degradation processes. After de-chlorination and de-alkylation, *S*-triazine ring is open as complete removal of atrazine.

#### 4. Conclusions

Atrazine is rapidly and completely degraded by microwave-assisted photocatalysis on TiO<sub>2</sub> nanotubes, the complete degradation of atrazine is obtained in 5 min and the mineralization ratio is 98.5% in 20 min. Atrazine, which is difficult to be mineralized by traditional AOPs, is effectively mineralized. The concentrations of Cl<sup>-</sup> and NO<sub>3</sub><sup>-</sup> increase gradually to 3, 27.8 mg/L, respectively. And the dates are close to their stoichiometric values. Five intermediates were detected, including EIST, OIET, ODET, HAET, and ADE. Among the intermediates, a new intermediate 2-hydroxy-4-ethylamino-6-isopropylamino-*S*-triazine (EIST) is detected. It may due to that C–Cl bond of atrazine is directly cleaved by the intense UV radiation generated by EDLs. These intermediates may be produced by direct photolysis or/and photocatalysis in MPC and both of photolysis and photocatalysis are responsible for the complete degradation of atrazine. Based on the efficient degradation and COD<sub>Cr</sub> removal of atrazine in MPC, microwave-assisted photocatalytic method

could be a potential technology to remove organic pollutants from waste waters.

#### Acknowledgments

The authors acknowledge the financial support from the Postdoctoral Nature Science Foundation of Jiangsu Province, China (0501010B) and Postdoctoral Nature Science Foundation of China (2005038238).

#### References

- [1] J.A. Erick, B.S. Mackay, E.T. Shane, E.S. Eric, Removal of atrazine from water using covalent sequestration, *J. Agric. Food Chem.* 52 (2004) 545–549.
- [2] R.D. Fallon, Evidence of a hydrolytic route for anaerobic cyanide degradation, *Appl. Environ. Microbiol.* 58 (1992) 3163–3164.
- [3] K. Banerjee, P.N. Cheremisinoff, S.L. Cheng, Sorption of organic contaminants by fly ash in a single solute system, *Environ. Sci. Technol.* 29 (1995) 2243–2251.
- [4] C.J. Somich, M.T. Muldoon, P.C. Kearney, On-site treatment of pesticide waste and rinate using ozone and biologically active soil, *Environ. Sci. Technol.* 24 (1990) 745–749.
- [5] G. Mascolo, A. Lopez, R. Foldenyi, R. Passino, G. Tiravanti, Prometryne oxidation by sodium hypochlorite in aqueous solution: kinetics and mechanism, *Environ. Sci. Technol.* 29 (1995) 2987–2991.
- [6] J. Arantegui, J. Prado, E. Chamarro, S. Eस्पugas, Kinetics of the UV degradation of atrazine in aqueous solution in the presence of hydrogen peroxide, *J. Photochem. Photobiol. A: Chem.* 88 (1995) 65–74.
- [7] S.M. Arnold, W.J. Hickey, R.F. Harris, Degradation of atrazine by Fenton's reagent: condition optimization and product quantification, *Environ. Sci. Technol.* 29 (1995) 2083–2089.
- [8] K. Ioannis, M. Konstantinou, Theophanis, Sakellarides, V. Sakkas, T. Albanis, Photocatalytic degradation of selected *S*-triazine herbicides and organophosphorus insecticides over aqueous TiO<sub>2</sub> suspensions, *Environ. Sci. Technol.* 35 (2001) 398–405.
- [9] E. Pelizzetti, V. Carlin, C. Minero, E. Pramauro, M. Vincenti, Degradation pathways of atrazine under solar light and in the presence of TiO<sub>2</sub> colloidal particles, *Sci. Total Environ.* 123–124 (1992) 161–169.
- [10] P. Sandra, E.S. Sarmiza, G. Isabel, T. Ravindranathan, Photocatalytic degradation of atrazine using suspended and supported TiO<sub>2</sub>, *Appl. Catal. B: Environ.* 51 (2004) 107–116.
- [11] C. Debabrata, D. Shimanti, Visible light induced photocatalytic degradation of organic pollutants, *J. Photochem. Photobiol. C* 6 (2005) 186–205.
- [12] C.C. Tsai, H. Teng, Regulation of the physical characteristics of titania nanotube aggregates synthesized from hydrothermal treatment, *Chem. Mater.* 16 (2004) 4352–4358.
- [13] S.G. Yang, X. Quan, X.Y. Li, Enhanced photocatalytic activity of nanotube-like titania by sulfuric acid treatment, *J. Environ. Sci.* 17 (2005) 290–297.
- [14] S. Horikoshi, H. Hidaka, N. Serpone, Environmental remediation by an integrated microwave/UV illumination technique, *J. Photochem. Photobiol. A: Chem.* 161 (2004) 221–225.
- [15] Z.H. Ai, P. Yang, X.H. Lu, Degradation of 4-chlorophenol by a microwave assisted photocatalysis method, *J. Hazard. Mater.* 124 (2005) 147–152.
- [16] C.C. Tsai, H. Teng, Structural features of nanotubes synthesized from NaOH treatment on TiO<sub>2</sub> with different post-treatments, *Chem. Mater.* 18 (2006) 367–373.
- [17] J. Hong, C. Sun, S.G. Yang, Y.Z. Liu, Photocatalytic degradation of methylene blue in TiO<sub>2</sub> aqueous suspensions using microwave powered electrodeless discharge lamps, *J. Hazard. Mater.* 133 (2006) 162–166.
- [18] S.G. Yang, Y.Z. Liu, C. Sun, Preparation of anatase TiO<sub>2</sub>/Ti nanotube-like electrodes and their high photoelectrocatalytic activity for the degradation of PCP in aqueous solution, *Appl. Catal. A* 301 (2006) 284–291.
- [19] S.G. Yang, X. Quan, X.Y. Li, C. Sun, Photoelectrocatalytic treatment of PCP in aqueous solution over rutile nanotube-like TiO<sub>2</sub>/Ti electrode, *Photochem. Photobiol. Sci.* 5 (2006) 808–814.

- [20] J. Zhao, T. Wu, K. Wu, K. Oikawa, H. Hidaka, N. Serpone, Photoassisted degradation of dye pollutants. 3. Degradation of the cationic dye Rhodamine B in aqueous anionic surfactant/TiO<sub>2</sub> dispersions under visible light irradiation: evidence for the need of substrate adsorption on TiO<sub>2</sub> Particles, *Environ. Sci. Technol.* 32 (32) (1998) 2394–2400.
- [21] S. Horihoshi, H. Hidaka, N. Serpone, Environmental remediation by an integrated microwave/UV-illumination method. 1. Microwave-assisted degradation of Rhodamine-B dye in aqueous TiO<sub>2</sub> dispersions, *Environ. Sci. Technol.* 36 (2002) 1357–1366.
- [22] C. Debabrata, M. Anima, Evidence of superoxide radical formation in the photodegradation of pesticide on the dye modified TiO<sub>2</sub> surface using visible light, *J. Photochem. Photobiol. A: Chem.* 165 (2004) 19–23.
- [23] G. Durand, D. Barcelo, J. Albaiges, M. Mansour, Utilisation of liquid chromatography in aquatic photodegradation studies of pesticides: a comparison between distilled water and seawater, *Chromatographia* 29 (1990) 120–124.
- [24] V. Hequet, C. Gonzalez, P. Le Cloirec, Photochemical processes for atrazine degradation: methodological approach, *Water Res.* 35 (2001) 4253–4260.
- [25] M. Pavel, K. Petr, C. Vladim'yr, The electrodeless discharge lamp: a prospective tool for photochemistry. Part 4. Temperature- and envelope material-dependent emission characteristics, *J. Photochem. Photobiol.* 158 (2003) 1–5.
- [26] L.B. Claudia, P. Carlo, R. Vittorio, S. Elena, Mechanism and efficiency of atrazine degradation under combined oxidation processes, *Appl. Catal. B: Environ.* 64 (2006) 131–138.
- [27] C.Y. Chan, S. Tao, R. Dawson, P.K. Wong, Treatment of atrazine by integrating photocatalytic and biological processes, *Environ. Pollut.* 131 (2004) 45–54.
- [28] J.F. Maria, I.F. Maria, M. Sixto, A.A. Jose, P. Jose, D. Xavier, Degradation of some biorecalcitrant pesticides by homogeneous and heterogeneous photocatalytic ozonation, *Chemosphere* 58 (2005) 1127–1133.
- [29] S. Horikoshi, H. Hidaka, Non-degradable triazine substrates of atrazine and cyanuric acid hydrothermally and in supercritical water under the UV-illuminated photocatalytic cooperation, *Chemosphere* 51 (2003) 139–142.
- [30] S. Kataoka, D.T. Tompkins, W.A. Zeltner, M.A. Anderson, Photocatalytic oxidation in the presence of microwave irradiation: observations with ethylene and water, *J. Photochem. Photobiol. A* 148 (2002) 323–330.
- [31] S. Horikoshi, H. Hidaka, N. Serpone, Environmental remediation by an integrated microwave/UV-illumination method. II. Characteristics of a novel UV-vis-microwave integrated irradiation device in photodegradation processes, *J. Photochem. Photobiol. A: Chem.* 153 (2002) 185–189.
- [32] Z.H. Ai, P. Yang, X.H. Lu, Degradation of 4-chlorophenol by microwave irradiation enhanced advanced oxidation processes, *Chemosphere* 60 (2005) 824–827.